X-ray diffraction and Mössbauer-effect study of the decagonal $Al_7(Mn_{1-x}Fe_x)_2$ alloy

B. Koopmans, P. J. Schurer,* and F. van der Woude
Solid State Physics Laboratory, University of Groningen, Groningen, The Netherlands

P. Bronsveld
Technical Physics Laboratory, University of Groningen, Groningen, The Netherlands
(Received 7 July 1986)

Ribbons of pure decagonal $Al_7(Mn_{1-x}Fe_x)_2$ $x=0$ and 0.3, have been prepared. The x-ray diffractogram has been indexed with a basis vector set that is closely related to the icosahedral set. A Mössbauer-effect study shows that the local iron environment in decagonal phase alloys is similar but less asymmetric than that in icosahedral alloys.

The icosahedral phase of Al-Mn alloys, first discovered by Shechtman *et al.*,[1] has a point-group symmetry $m\,\bar{3}\,\bar{5}$ that is nonperiodic in all directions. More recently, Bendersky[2] showed that the "*T*-phase" Al-Mn alloy[3] has also a noncrystallographic point group $10/m$ or $10/mmm$. However, this phase has translational symmetry in one dimension. The icosahedral Al-Mn phase always coexists with the decagonal *T* phase and fcc Al. By addition of small amounts of Si, the *T* phase is suppressed and only the icosahedral phase remains.[4]

In this contribution we discuss the preparation of the pure decagonal phase and the results of an angular dispersive x-ray diffraction (ADXD) study and a Mössbauer-effect (ME) study.

Decagonal alloys were prepared by using the melt-spin technique. Molten alloys of composition Al_7Mn_2 and $Al_7(Mn_{0.7}Fe_{0.3})_2$ were rapidly quenched in argon atmosphere onto the outer surface of a rotating wheel. Ribbons of about 1 mm wide and 25 μm thick were obtained. The ribbons were annealed at about 550 K to remove lattice defects. Subsequently, transmission electron microscopy (TEM) studies showed that the diffraction patterns for both samples agreed with those published by Bendersky.[2]

The ADXD diffractogram of decagonal $Al_7(Mn_{0.7}Fe_{0.3})_2$ is represented in Fig. 1. No indication of fcc Al is found in the diffractogram. The diffraction patterns of quasicrystalline materials can be indexed by using the projection method.[5] For icosahedral quasicrystals the diffraction peaks can be indexed by using a set of six vectors $\{q_n^0\}$ that together with six opposite ones are the vertex vectors of an icosahedron, $\mathbf{q}_0^0=q_i\hat{\mathbf{z}}$, $\mathbf{q}_n^0=q_i[(\cos\theta)\hat{\mathbf{z}}+(\sin\theta R^n)\hat{\mathbf{x}}]$, $n=1$ to 5, where $\cos\theta=1/\sqrt{5}$ and $R=2\pi/5$.

According to Ho[6] the decagonal diffraction pattern can be indexed by a set $\{q_n\}$ that is closely related to the icosahedral set:

$$\mathbf{q}_0=2q_d(\cos\alpha)\hat{\mathbf{z}},\quad \mathbf{q}_n=q_d[(\cos\alpha)\hat{\mathbf{z}}+(\sin\alpha R^n)\hat{\mathbf{x}}]\ ,\qquad n=1\text{ to }5\ .$$

The vectors $\{q_n\}$ and $\{q_0-q_n\}$ are the lower and upper edges, respectively, of a pentagonal pyramid. The translational symmetry is in the *z* direction.

We will call the *z* component of a vector of the crystalline component and its component in the *xy* plane the quasicrystalline component. The set $\{q_n\}$ does not determine uniquely the indices of the diffraction pattern in Fig. 1. This is so, firstly because $5\mathbf{q}_0=\sum_{n=1}^{5}\mathbf{q}_n$, and secondly because basis sets are equivalent if the quasicrystalline-components differ only in the power of τ. Here τ is the golden mean, $(1+\sqrt{5})/2$.

Elser[5] has shown that quasicrystal diffraction patterns can be conveniently analyzed by using inflation and deflation matrices. For the case of the decagonal diffraction pattern we introduce the inflation transformation matrix

$$M_{ij}=\begin{bmatrix}1&1&0&0&1\\1&1&1&0&0\\0&1&1&1&0\\0&0&1&1&1\\1&0&0&1&1\end{bmatrix}$$

for transforming the subset $\{q_n\}$, $n=1$ to 5. M_{ij} multiplies the quasicrystalline component of a vector by a factor τ.

All the strongest peaks in the ADXD diffractogram (Fig. 1) can be indexed by using only inflations of the type $M_{ij}^p(r^n\mathbf{q}_1)$ or $M_{ij}^p(R^n(\mathbf{q}_1-\mathbf{q}_2))$. This results in quasicrystalline components of, respectively, $\tau^p q_d\sin\alpha$ and $\tau^p r q_d\sin\alpha$, where *p* and *n* are integers and $r=2\sin(\pi/5)$. The quasicrystalline components may have to be combined with a crystalline component, i.e., a combination of $\mathbf{q}_0$ and $\sum_{n=1}^{5}\mathbf{q}_n$.

The *q* values corresponding to the peak positions in the diffractogram of $Al_7(Mn_{0.7}Fe_{0.3})_2$ are shown in Table I. By indexing the $q=3.078$ Å^{-1} peak as $(0\ 12\bar{0}1)$, the indexing scheme shown in Table I follows. A weak peak at $q=4.135$ Å^{-1} is the only peak that cannot be indexed by the two inflation rules described above. However, it can be fitted in by a threefold inflation of $R^n(\mathbf{q}_1+\mathbf{q}_2-\mathbf{q}_4)$.

The experimental *q* values of decagonal $Al_7(Mn_{0.7}Fe_{0.3})_2$ have been least-squares fitted by using the crystalline component $q_d\cos\alpha$ and the quasicrystalline

component $q_c \sin\alpha$ as free parameters. For $q_d \sin\alpha = 0.6163(3)$ Å^{-1} and $q_d \cos\alpha = 0.5067(7)$ Å^{-1}, we obtain the theoretical q values shown in Table I. A fit of the experimental q values of icosahedral Al-($Mn_{0.7}Fe_{0.3}$) gives $q_i \sin\theta = 0.6159(10)$.[7] We conclude that the icosahedral and decagonal components in the xy plane are the same within the experimental uncertainty.

The ADXD diffractogram of decagonal Al_7Mn_2 can be indexed in the same way. We obtain $q_d \sin\alpha = 0.6142(5)$ Å^{-1} and $q_d \cos\alpha = 0.5053(5)$ Å^{-1}. Again, the quasicrystalline component in decagonal Al_7Mn_2 agrees with the corresponding value $q_i \sin\theta = 0.6132(5)$ Å^{-1} in the icosahedral structure of the Al-Mn alloy. Since all diffraction peaks can be fitted with the decagonal indexing scheme and the ribbons do not contain Al, the stoichiometry of decagonal Al-Mn alloys corresponds with Al_7Mn_2.

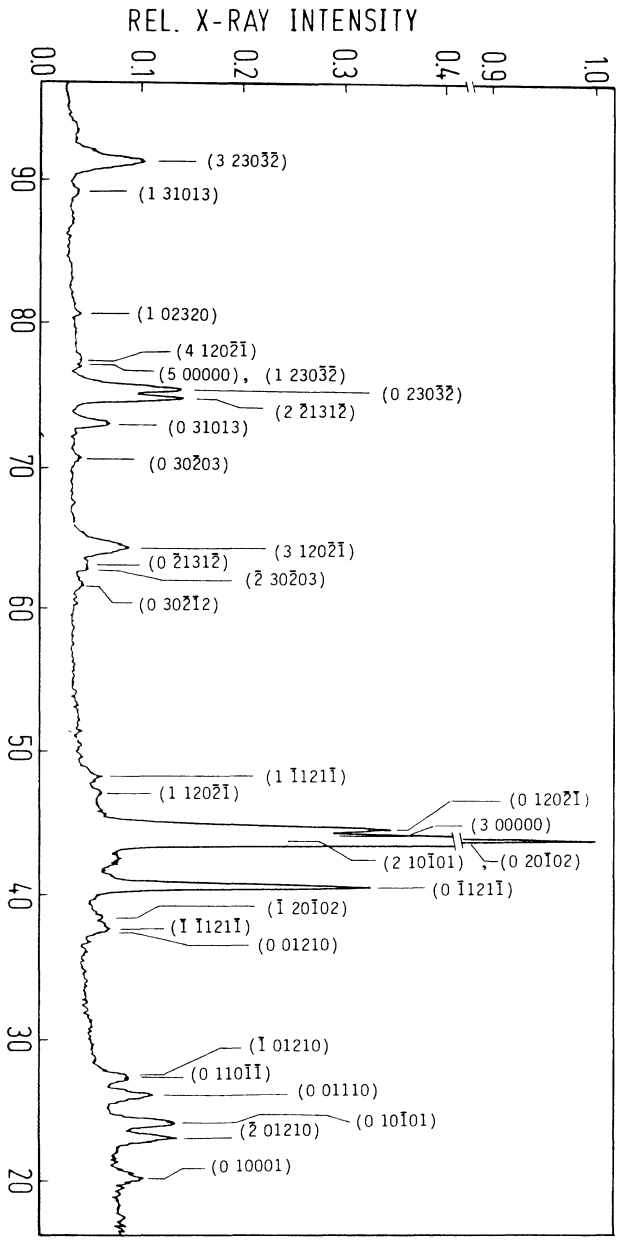

FIG. 1. X-ray diffraction pattern of decagonal $Al_7(Mn_{0.7}Fe_{0.3})_2$. Labels are the Miller indices as discussed in the text.

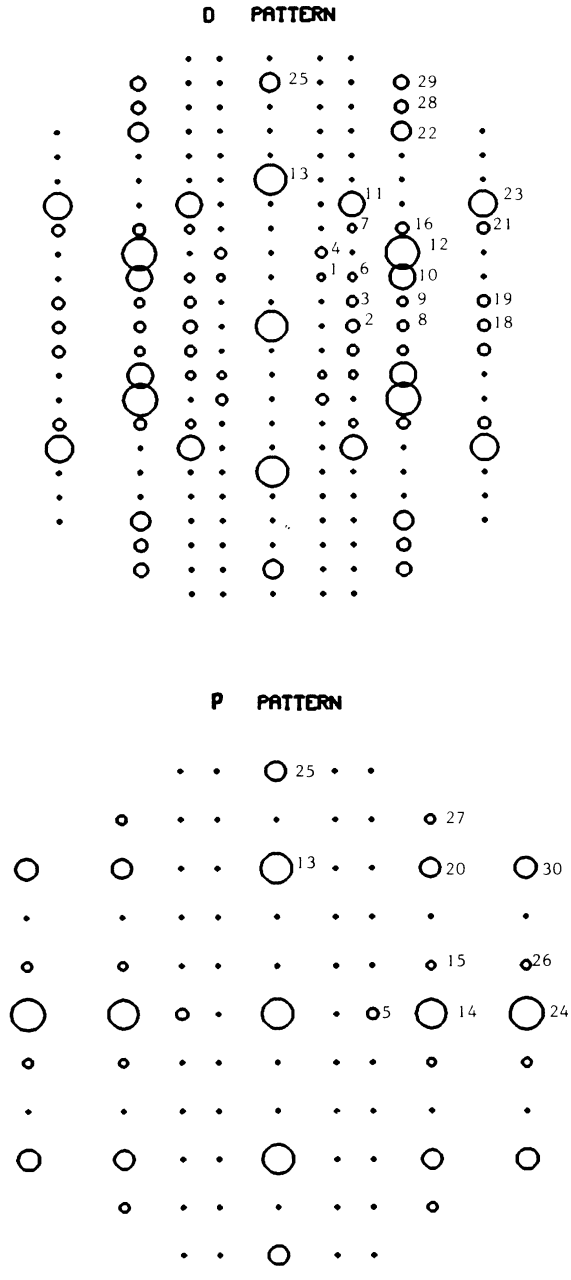

FIG. 2. Laue diffraction patterns along the pentagonal and decagonal zone axes constructed by using the information shown in Fig. 1. The intensities are proportional to the third power of the radii of the circles. The numerals refer to the listing of the peaks in Table I. The smallest spots are not detected in Fig. 1. The crystalline direction is vertical in the two plots.

TABLE I. The indexing scheme, symmetry planes, quasicrystalline (qc) components (in units of $q_d \sin\alpha$), and the experimental and theoretical **q** values for decagonal $Al_7(Mn_{0.7}Fe_{0.3})_2$, $\tau=(1+\sqrt{5})/2$ and $r=2\sin(\pi/5)$. The label numbers refer to the Laue spots shown in Fig. 2.

Index	Plane	qc component	q_{theor} (Å^{-1})	q_{expt} (Å^{-1})	Label
(0 10001)	D	τ	1.422	1.419	1
($\bar{2}$ 01210)	10,D	τ^2	1.614	1.615	2
(0 10$\bar{1}$01)	D	τ^2	1.691	1.689	3
(0 01110)	D	τ	1.818	1.821	4
(0 110$\bar{1}$ $\bar{1}$)	10,P	$\tau^2 r$	1.897	1.904	5
($\bar{1}$ 01210)	D	τ^2	1.905		6
(0 01210)	D	τ^2	2.591	2.607	7
($\bar{1}$ $\bar{1}$121$\bar{1}$)	10,D	τ^3	2.611		8
($\bar{1}$ 20$\bar{1}$02)	D	τ^3	2.660	2.662	9
(0 $\bar{1}$121$\bar{1}$)	D	τ^3	2.801	2.801	10
(2 10$\bar{1}$01)	D	τ^2	3.004		11
(0 20$\bar{1}$02)	D	τ^3	3.021	3.024	12
(3 00000)	D,P	0	3.040		13
(0 120$\bar{2}$ $\bar{1}$)	10,P	$\tau^3 r$	3.069	3.078	14
(1 120$\bar{2}$ $\bar{1}$)	P	$\tau^3 r$	3.232	3.237	15
(1 $\bar{1}$121$\bar{1}$)	D	τ^3	3.305	3.309	16
(0 30$\bar{2}$ $\bar{1}$2)			4.155	4.156	17
($\bar{2}$ 30$\bar{2}$03)	10,D	τ^4	4.224	4.219	18
(0 $\bar{2}$131$\bar{2}$)	D	τ^4	4.255	4.253	19
(3 120$\bar{2}$ $\bar{1}$)	P	$\tau^3 r$	4.320	4.324	20
(0 30$\bar{2}$03)	D	τ^4	4.685	4.685	21
(0 31013)	D	τ^3	4.822	4.822	22
(2 $\bar{2}$131$\bar{2}$)	D	τ^4	4.926	4.920	23
(0 230$\bar{3}$ $\bar{2}$)	10,P	$\tau^4 r$	4.966	4.962	24
(5 00000)	D,P	0	5.067		25
(1 230$\bar{3}$ $\bar{2}$)	P	$\tau^4 r$	5.068	5.070	26
(4 120$\bar{2}$ $\bar{1}$)	P	$\tau^3 r$	5.084		27
(1 02320)	D	τ^3	5.255	5.262	28
(1 31013)	D	τ^3	5.700	5.705	29
(3 230$\bar{3}$ $\bar{2}$)	P	$\tau^4 r$	5.813	5.823	30

For icosahedral Al-M alloys, where M is a $3d$ transition element, the icosahedral structure contracts as the number of $3d$ electrons increases.[7] Apparently, this is also the case for the decagonal structure since the q values for this structure change in the same manner.

TEM diffractograms of the decagonal phase show one tenfold and ten equivalent twofold decagonal (D) patterns. The angle between the tenfold axis and the D-zone axes is 90° and the angle between two adjacent D-zone axes is 36°. Ten equivalent twofold pentagonal (P) patterns of a type different from the D pattern are found with the P-zone axes situated midway between adjacent D-zone axes.[2,8]

We have constructed the Laue patterns along the P- and D-zone axes for $q<5.9$ Å^{-1} by using the intensities of the ADXD peaks after correction with the Lorentz polarization factor and the multiplication factor. For overlapping peaks in the ADXD diffractogram the intensity distribution in the Laue pattern has been taken from the TEM diffractogram.[8] The diffraction spots derived from inflations of the type $R^n\mathbf{q}_1$ will give D patterns, and spots derived from inflation of $R^n(\mathbf{q}_1-\mathbf{q}_2)$ will give P patterns (see also Table I). The Laue patterns shown in Fig. 2 are in good agreement with the TEM diffractograms of D and P patterns.

The ME spectrum of decagonal $Al_7(Mn_{0.7}Fe_{0.3})_2$ is shown in Fig. 3. For the purpose of comparison with the ME studies of the icosahedral phase,[9–11] we will discuss a fit with two components. The two doublets have a linewidth $\Gamma=0.29$ mm/s and an area ratio $D_1/D_2=1.5$,

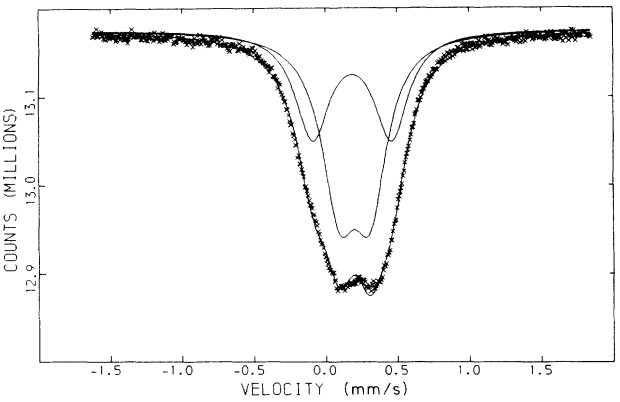

FIG. 3. Mössbauer spectrum of decagonal $Al_7(Mn_{0.7}Fe_{0.3})_2$.

where D_1 has the smaller quadrupole splitting. The area ratio is close to the golden mean value 1.618 which may support the possibility that iron sites may be divided into two groups that correspond to decorations of oblate and prolate rhombohedra. A quasiperiodic structure can be generated that fills all space, if the two polyhedra occur in a ratio 1.618.[12] Other possible explanations for a distribution of iron sites are (a) the occurrence of vacancies at Al positions[11] and (b) a decagonal structure that consists of Mackay icosahedra.[7] The two doublets have isomer shift values $\Delta_1=0.20$ mm/s and $\Delta_2=0.19$ mm/s that are very close but slightly lower than those for icosahedral Al-($Mn_{0.7}Fe_{0.3}$) alloys ($\Delta_1=0.22$ mm/s and $\Delta_2=0.21$ mm/s). This result suggests that, as in the case of icosahedral alloys,[7] the Fe atoms in decagonal alloys are located in a strain free structure of nearest-neighbor Al atoms. The two doublets have quadrupole splitting values $\delta_1=0.22$ mm/s and $\delta_2=0.55$ mm/s. Whereas the large δ value agrees with the value found for the smaller component in icosahedral Al-($Mn_{0.7}Fe_{0.3}$) alloys, the δ value of the doublet with the largest intensity is significantly smaller than the corresponding icosahedral doublet.

In summary, the ME study shows that the local structure around Fe atoms in decagonal and icosahedral alloys is similar. However, for a large number of Fe atoms the local structure is less asymmetric in the decagonal structure.

This investigation forms part of the FOM-program. Stichting voor Fundamenteel Onderzoek der Materie (Utrecht, The Netherlands) (FOM) program.

---

*Present address: Royal Roads Military College, F.M.O. Victoria, British Columbia, Canada, V0S 1B0.

[1]D. Shechtman, I. Blech, D. Gratias, and J. W. Cahn, Phys. Rev. Lett. **53**, 1951 (1984).

[2]L. Bendersky, Phys. Rev. Lett. **55**, 1461 (1985).

[3]L. Bendersky, R. J. Schaefer, F. G. Biancanniello, W. J. Boettinger, M. J. Kaufman, and D. Shechtman, Scr. Metall. **19**, 919 (1985).

[4]C. H. Chen and H. S. Chen, Phys. Rev. B **33**, 2814 (1986).

[5]V. Elser, Phys. Rev. B **32**, 4892 (1985).

[6]Tin-Lun Ho, Phys. Rev. Lett. **56**, 468 (1986).

[7]P. J. Schurer, B. Koopmans, and F. van der Woude (unpublished).

[8]K. K. Fung, C. Y. Yang, Y. Q. Zhou, J. G. Zhao, W. S. Zhan, and B. G. Shen, Phys. Rev. Lett. **56**, 2060 (1986).

[9]L. J. Swartzendruber, P. Shechtman, L. Bendersky, and J. W. Cahn, Phys. Rev. B **33**, 7314 (1986).

[10]M. Eibschutz, H. G. Chen, and J. J. Hansen, Phys. Rev. Lett. **56**, 169 (1986).

[11]P. J. Schurer, B. Koopmans, F. van der Woude, and P. Bronsveld, Solid State Commun. **59**, 619 (1986).

[12]D. Levine and P. J. Steinhardt, Phys. Rev. Lett. **53**, 2477 (1984).